Measurements of the density-temperature cross-phase angle of turbulent fluctuations at ASDEX-Upgrade and comparison to theory

S.J. Freethy[1], C. Lechte[2], P. Rodriguez-Fernandez[3], E. Fable[4], T. Goerler[4], G.D. Conway[4], A.J. Creely[3], T. Happel[4], P. Hennequin[5], A.E. White[3] and the ASDEX Upgrade team

[1]*United Kingdom Atomic Energy Authority, Culham Centre for Fusion Energy, Culham Science Centre, Abingdon, Oxon, OX14 3DB, UK.*

[2]*Universität Stuttgart, Institut für Grenzflächenverfahrenstechnik und Plasmatechnologie IGVP, 70569 Stuttgart, Germany*

[3]*Plasma Science and Fusion Center, Massachusetts Institute of Technology, Cambridge, MA 02139, USA*

[4]*Max Plank Institute for Plasma Physics, 85748 Garching, Germany*

[5]*Laboratoire de Physique des Plasmas, Ecole Polytechnique, 91128, Palaiseau cedex, France*

Introduction

The experimental validation of turbulence models is a critical part of developing a predictive understanding of plasma transport. Models based on the non-linear gyrokinetic equations are currently the most well understood and experimentally validated models of turbulence available. However, models of reduced complexity are required in order to make useful transport predictions for future machines. Development of such models has made steady progress, however, there has not been extensive validation of these models against measured turbulent quantities and their trends. It is interesting to compare model predictions, where available, for turbulent quantities which are directly related to the heat flux, such as fluctuation amplitudes and cross-phase angles of fluctuating quantities. The most experimentally accessible cross-phase quantity is that between the temperature and density fluctuations α_{nT}, and this has previously been demonstrated using a reflectometer for the density fluctuation information and a radiometer for temperature fluctuation information [1, 2, 3].

Experiment

At ASDEX Upgrade, an F-band (100-130 GHz) multi-channel ECE diagnostic is combined with two W-band and one V-band reflectometers along the same line of sight. In practice, the radial alignment of these diagnostics must be within a radial correlation length, which at ASDEX Upgrade is 1-2 cm, to ensure a large enough cross-correlation can be achieved to overcome the thermal noise in the ECE emission. The uncertainty of the density profile makes radial alignment to within the required tolerance difficult and time consuming to achieve. We may equally consider this uncertainty as an uncertainty in the frequency of the radially matched ECE radiation for which a bandwidth of 5 GHz is sufficient to cover the uncertainty in the reflectometer

position. Thus at ASDEX Upgrade, a 28 channel comb with either 125 or 250 MHz spacing was designed [4], so that the diagnostic cross correlation has a higher chance of success. This diagnostic was also used for Cross Correlation ECE measurements of temperature fluctuations $\tilde{T}_{e\perp}$.

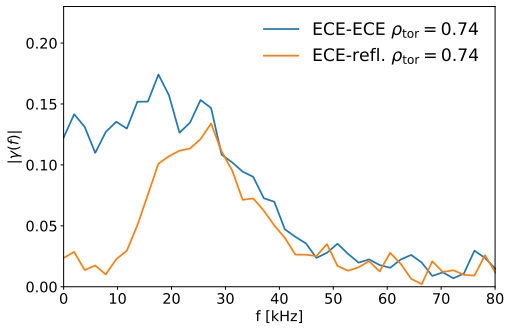

Figure 1: (orange) shows coherence between reflectometer amplitude fluctuations and closest ECE channel, while (blue) shows coherence of 2 adjacent CECE channels.

Figure 1 shows the cross-coherence, γ, of two neighbouring ECE channels, representing the temperature fluctuation spectrum. Also shown is the cross-coherence of ECE and reflectometer amplitude fluctuations. There is a clear difference in the spectra at low frequency, giving the appearence of a quasi-coherent mode. This is in fact due to the loss of information of low k density fluctuations in the amplitude fluctuations, as will now be shown.

Reflectometer Modelling

To correctly interpret the measurement of the cross-phase, α_{nT}, it is essential that a thorough understanding of how the reflectometer preserves or transforms the absolute phase of the density fluctuations in both the measured signal amplitude, $A = I^2 + Q^2$, and signal phase, $\phi = \arctan Q/I$. Reflectometer cross-correlation has been studied in detail in the linear and non-linear regimes [5, 6]. However these studies focussed on cross-correlation of two reflectometer signals and do not highlight the relative phase angle between A, ϕ and $\tilde{n}$, essential for the present work. Thus we attempt to address these aspects here. Cross-correlation of these quantities with $\tilde{n}$ was initially studied by utilising full wave calculations performed with the IPF-FD3D code [7], using a turbulent density field generated by the GENE gyrokinetic code [8] based on the ECRH heated L-mode plasma described in [9]. The nominal $\tilde{n}/n$ from GENE was 0.62% and this produced a nonlinear reflectometer response in the simulations. The turbulence was scaled by 0.1, 0.5 and 1.0 to generate a range of responses from linear to non-linear. It was found by cross-correlating the simulated reflectometer signal with the density perturbations, that ϕ was in phase with $\tilde{n}$ for low $\tilde{n}/n$, however coherence was unmeasurable at realistic $\tilde{n}/n$ for this set-up. By contrast, A remained coherent with $\tilde{n}$, even in the non-linear regime of the

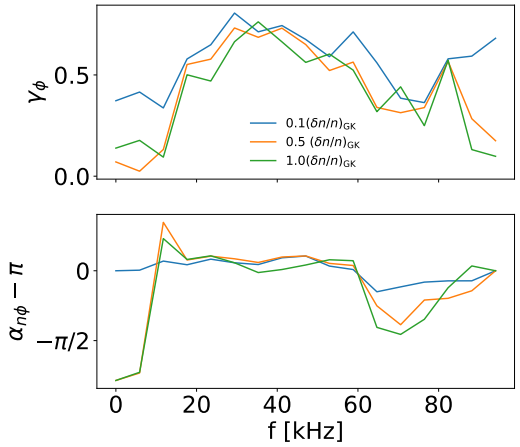

Figure 2: The cross-coherence of reflectometer amplitude fluctuations with the original density perturbations.

reflectometer response, as shown by Figure 2. For the AUG experiential set-up, A was found to be out of phase with $\tilde{n}$, however this is not universal. An analytic model for the reflectometer response, based on the Born approximation was found to be useful in elucidating the behaviour of ϕ and A. It can be shown from the Born approximation, using the reciprocity theorem to calculate the reflectometer scattered signal response [10] and by only considering 1D perturbations of the form $\cos(\Omega t - k_p x)$ just inside the cut-off, that the scattered reflectometer signal s has the relationship

$$s \propto i \frac{\exp\left[-\left(\frac{k_p w}{2\sqrt{2}}\right)^2 \frac{1}{1-i\beta}\right]}{\sqrt{1-i\beta}} \cos(\Omega t), \tag{1}$$

where $\beta = k_0 w^2 / R_{\text{eff}}$, w is the $1/e$ electric field radius at the perturbation and R_{eff} is the effective radius of curvature beteween the cut-off surface and the wavefronts, $1/R_{\text{eff}} = 1/\rho_{(wavefront)} + 1/\rho_{(cutoff)}$. ρ_x is positive for wavefronts diverging from the antenna.

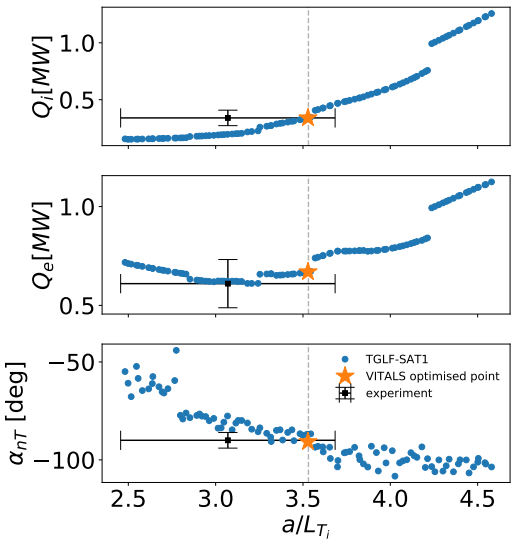

Figure 3: Experimental results (black), and TGLF-SAT1 (blue) results for ion heat flux, electron heat flux and α_{nT}. VITALS optimised point shown in orange.

Using this model it is possible to show that the cross-phase of $\tilde{n}$ and ϕ depends upon the perturbation wavenumber, k_p, being alternately in and out of phase with $\tilde{n}$ for increasing k_p. At $k_p = 0$, ϕ is always in phase with $\tilde{n}$. The cross-phase between $\tilde{n}$ and A shows a similar behaviour and additionally depends on the sign of the effective curvature, being π for $R_{\text{eff}} < 0$ and 0 for $R_{\text{eff}} > 0$. Both the full wave simulations and the Born approximation model show a reduction in the coherence between $\tilde{n}$ and A at low frequency/k and this is primarily due to the doubling of the frequency of these perturbations in A originating from a beam swinging behaviour, which is well documented [11].

TGLF Comparisons

The measurements of α_{nT} were made in an AUG ECRH heated L-mode plasma described in [9] and compared to non-linear gyrokinetic simulations made using GENE. These comparisons are now extended to the reduced model TGLF-SAT1, where an average α_{nT} is calculated using

$$\alpha_{nT,\text{TGLF}}(k_y) = \arctan\left[\frac{\text{Re}\{[n(k_y)T^*_{e\perp}(k_y)]_1 + [n(k_y)T^*_{e\perp}(k_y)]_2\}}{\text{Im}\{[n(k_y)T^*_{e\perp}(k_y)]_1 + [n(k_y)T^*_{e\perp}(k_y)]_2\}}\right], \tag{2}$$

where the subscript 1 and 2 refer to the dominant and first subdominant mode respectively. In this case the Ion Temperature Gradient (ITG) mode and Trapped Electron Mode (TEM). These

two modes have distinct α_{nT} which tend to be unchanged from the linear to non-linear state, and for plasmas close to the transition from dominant ITG to dominant TEM, the saturated turbulent state contains a mix of these modes. The resulting average α_{nT} thus lies in between the linear values of α_{nT} of the two modes. Figure 3 shows the average α_{nT} given by Equation (2) when scanning the normalised ion temperature gradient a/L_{T_i}, driving the ITG instability. As can be seen, good agreement can be found between TGLF and experiment for all three of Q_i, Q_e and α_{nT} within the uncertainty of the inputs. A simulation point matching the experimental constraints is found by reducing a/L_{T_e} by 15%, increasing a/L_{T_i} by 17% and decreasing a/L_n by <1% and an optimisation framework for the validation of transport codes, VITALS [12], was used to find the values for a/L_{T_i} and a/L_n. Since the ion mode is predominantly responsible for the ion heat flux and the electron mode for the electron heat flux, it is encouraging that the TGLF-SAT1 model is capable of matching all three parameters to experiment, suggesting a realistic ratio of saturated amplitudes of ITG and TEM to reproduce the experimental heat fluxes.

Acknowledgements

This work has been carried out within the framework of the EUROfusion Consortium and has received funding from the Euratom research and training programme 2014-2018 and 2019-2020 under grant agreement No 633053. The views and opinions expressed herein do not necessarily reflect those of the European Commission. This work was also performed within the framework of the Helmholtz Virtual Institute on Plasma Dynamical Processes and Turbulence Studies using Advanced Microwave Diagnostics.

References

[1] M. Häse, M. Hirsch, H. J. Hartfuss, *Review of Scientific Instruments* **70**, 1014 (1999).

[2] A. E. White, *et al.*, *Physics of Plasmas* **17**, 056103 (2010).

[3] J. Hillesheim, *et al.*, *Physical Review Letters* **110**, 045003 (2013).

[4] A. J. Creely, *et al.*, *Review of Scientific Instruments* **89**, 053503 (2018).

[5] E. Z. Gusakov, B. O. Yakovlev, *Plasma Physics and Controlled Fusion* **44**, 2525 (2002).

[6] E. Z. Gusakov, A. Y. Popov, *Plasma Physics and Controlled Fusion* **46**, 1393 (2004).

[7] C. Lechte, G. D. Conway, T. Görler, C. Tröster-Schmid, *Plasma Physics and Controlled Fusion* **59**, 075006 (2017).

[8] F. Jenko, W. Dorland, *Plasma Physics and Controlled Fusion* **43**, A141 (2001).

[9] S. J. Freethy, *et al.*, *Physics of Plasmas* **25**, 055903 (2018).

[10] A. D. Piliya, A. Y. Popov, *Plasma Physics and Controlled Fusion* **44**, 467 (2002).

[11] G. Conway, *3rd Intl. Reflectometer Wksp. for Fusion Plasmas (Madrid), ITC 383* (1997), pp. 39–47.

[12] P. Rodriguez-Fernandez, *et al.*, *Fusion Science and Technology* **74**, 65 (2018).